# MULTISCALE SIMULATION OF SHORT FIBER REINFORCED PLASTICS FOR HYBRID COMPOSITES

André Hürkamp[1], Tobias Gebken[1], Anke Müller[1] and Klaus Dröder[1]

[1] TU Braunschweig, Institute of Machine Tools and Production Technology,
Langer Kamp 19b, 38106 Braunschweig, Germany
Email: a.huerkamp@tu-braunschweig.de, t.gebken@tu-braunschweig.de,
a.mueller@tu-braunschweig.de, k.droeder@tu-braunschweig.de
Web Page: https://www.tu-braunschweig.de/iwf/

**Keywords:** Multiscale Simulation, SFRP, Injection Molding, Multimaterial Composites

**Abstract**
In this contribution, a multiscale approach for the simulation of short fiber reinforced plastics (SFRP) is presented. We propose a virtual process chain in order to take into account the resulting fiber orientation obtained from fill simulations for the structural analysis. For the stress analysis of SFRP components, an anisotropic elasto-plastic material model is parametrized. Finally, multiscale simulations of a SFRP component under bending load are carried out and validated by experiments. In addition, a concept for the integrated manufacturing of hybrid composites bonded by form closure effects is presented.

## 1. Introduction

In nowadays lightweight car concepts, hybrid composites made up of a combination of metal and thermoplastic composites are promising multimaterial solutions to enable weight-reduced and efficient line production in the automotive industry. However, introducing lightweight components as load carrying parts, numerical tools are required to describe the mechanical behavior of these composites based on their micromechanics. An accurate material description taking into account non-linear effects and anisotropy due to the manufacturing process is mandatory to estimate the strength and durability of composites. Sophisticated simulation tools enable the identification of new potentials for lightweight parts. In this contribution, the virtual process chain for short fiber reinforced plastics is described and validated. It consists of three main methods, the process simulation of the injection molding process, the mapping of field variables such fiber orientation on the structural component as well as the structural analysis taking into account process-induced anisotropic and inhomogeneous material properties. Finally, the multiscale approach is validated by experimental tests.

The experimental investigations contain the manufacturing process of fiber reinforced plastic test specimens for the characterization of tensile modulus and tensile strength. The manufacturing process of fiber reinforced plastics affects the fiber orientation during the melt flowing process. Among others, flow direction, cavity geometry and shear effects through friction affected by temperature gradients between mold surface and melt are influencing the fiber orientation. Therefore, the material parameters of the fiber reinforced plastics are evaluated for different glass fiber mass fractions and different fiber orientations on an idealized plate geometry and are transferred to a structural model consisting of a complex threedimensional geometry.

## 2. Material Characterization

For the material characterization, the fiber reinforced plate geometry shown in Figure 1 is fabricated. The plate geometry consists of two parts: on the right hand side, testing specimens can be cut out to evaluate the effects of fiber orientation. On the left hand side, a specimen with a weld line in the center of the gauge section is obtained due to the melt flow. The plate has a constant thickness of 2 mm.

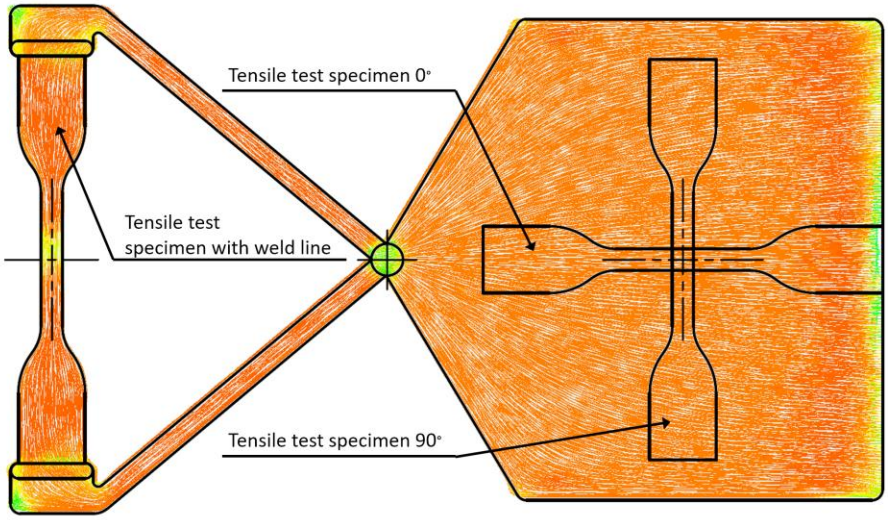


**Figure 1.** Computed fiber orientation in the plate geometry and positions of the specimens.

### 2.1. Experimental Investigations

The injection molding process is performed using the process parameters of Table 1. Two different short glass fiber mass fractions of 30% and 50% included in a polyamide 6 thermoplastic matrix are taken into accountconsidered. For the experiments, an injection molding machine ENGEL Victory 120 with maximum clamp pressure of 120 tons is used. The melt temperature is adjusted to 280 °C and 290 °C at the nozzle, the last heating unit before the melt is running into the mold. The injection speed and the holding pressure are constant during the experiments.

**Table 1.** Injection molding process parameter

| Material | Tool Temperature (°C) | Melt Temperature (°C) | Injection Speed ($cm^3/s$) | Holding Pressure (bar) |
|---|---|---|---|---|
| PA6 GF30 | 100 | 280 | 25 | 400 |
| PA6 GF50 | 100 | 290 | 25 | 400 |

The tensile test specimen geometry (DIN EN ISO 527-4 Typ 5A) has a length of 75 mm, a width of 12.5 mm at the clamping area and a width of 4 mm at the gauge section, as well as a constant thickness of 2 mm. For the material data fitting, specimens are cut out of the plate in the flow direction of 0° and 90° in order to obtain specimens with a mainly longitudinal (0°) and transversal (90°) fiber orientation. The tensile experiments are carried out at a testing speed of 5 mm/min.

## 2.2. Material Modelling and Parameter Fitting

For the multiscale analysis of short fiber reinforced thermoplastics, the microstructure needs to be considered for an accurate stress analysis at the structural level. The different scales are linked by analytical and computational homogenization schemes, respectively. In particular, analytical homogenization schemes are well suited for the analysis of SFRP since they exhibit accurate results and small computational effort.

In the literatureother research, several analytical homogenization methods and bounds for effective material properties exist [1]. In general, such schemes are based on the Eshelby solution [2], which provides an analytical solution for the stress field at the microstructure with ellipsoidal inclusion. In this contribution, we use the Mori-Tanaka method [3] since the computational effort is low and it has shown good agreement with experimental observations for the calculation of effective material properties [4]. It is implemented into the nonlinear, multiscale material and structural modeling software DIGIMAT, using a two-step mean field homogenization procedure for a composite with misaligned inclusion [5]. In case of SFRP, the microstructure consists of two phases: inclusion and matrix. The inclusion phase is described by an elastic material representing short glass fibers. The elastic material constants and the fibers aspect ratio *a* are given in Table 2.

**Table 2.** Elastic material constants of the glass fibers

| Young's Modulus (MPa) | Poisson's Ratio (-) | Apect Ratio (-) |
|---|---|---|
| 72000 | 0.22 | 22 |

The orientation of the glass fibers within the specimen is described by the fiber orientation tensor $\boldsymbol{a}$ obtained from rheological simulations. The thermoplastic matrix material consists of polyamide 6. For the quasi-static analysis, we use an elasto-plastic material formulation. The plastic behavior is described by $J_2$-plasticity, where a equivalent stress

$$\sigma_{\mathrm{eq}} = \sqrt{J_2(\boldsymbol{\sigma})} = \sqrt{\frac{3}{2}\boldsymbol{s} : \boldsymbol{s}} \tag{1}$$

is derived from the second invariant of the deviatoric stress tensor

$$\boldsymbol{s} = \boldsymbol{\sigma} - \frac{1}{3}\mathrm{Tr}(\boldsymbol{\sigma})\mathbf{I}. \tag{2}$$

Furthermore, isotropic hardening is assumed using the hardening function

$$Y(p) = H_{iso}\, p + Y_\infty \left[1 - \exp(-\beta\, p)\right] \tag{3}$$

to describe the mechanical behavior after plastic deformations are present. In Eq. (3), the linear hardening modulus $H_{iso}$, the hardening modulus $Y_\infty$, and the hardening exponent $\beta$ are material parameters, that are to be determined in accordance with experimental data. The history variable $p$ describes the accumulated plastic strain. During the finite element analysis, the yield function

$$f(\boldsymbol{\sigma}, Y) = \sigma_{\mathrm{eq}} - \sigma_y - Y(p) \leq 0 \tag{4}$$

is evaluated, where $\sigma_y$ describes the yield stress. Thus, plastic deformation can only occur when Eq. (4) is violated. Consequently, in combination with the elastic constants, six material parameters are to be determined for this composite material. Here, we use a reverse engineering approach. The material parameters are fit to the experimental data from the tensile tests in section 2.1 by mathematical optimization. The resulting material parameters for the two investigated materials PA6GF30 and PA6GF50 are listed in Table 3. Figure 2 depicts the experimental and fitted uniaxial material responses. The used material formulation shows excellent agreement with the experimental data.

**Table 3.** Material properties of the investigated SFRP

| Material | Young's Modulus (MPa) | Poisson's Ratio (-) | Yield stress (MPa) | Linear Hardening Modulus (MPa) | Hardening Modulus (MPa) | Hardening Exponent (-) |
|---|---|---|---|---|---|---|
| PA6GF30 | 2452.2 | 0.37 | 14.32 | 17.5 | 60.3 | 75 |
| PA6GF50 | 2136.6 | 0.37 | 9.528 | 83.5 | 61.9 | 50.9 |

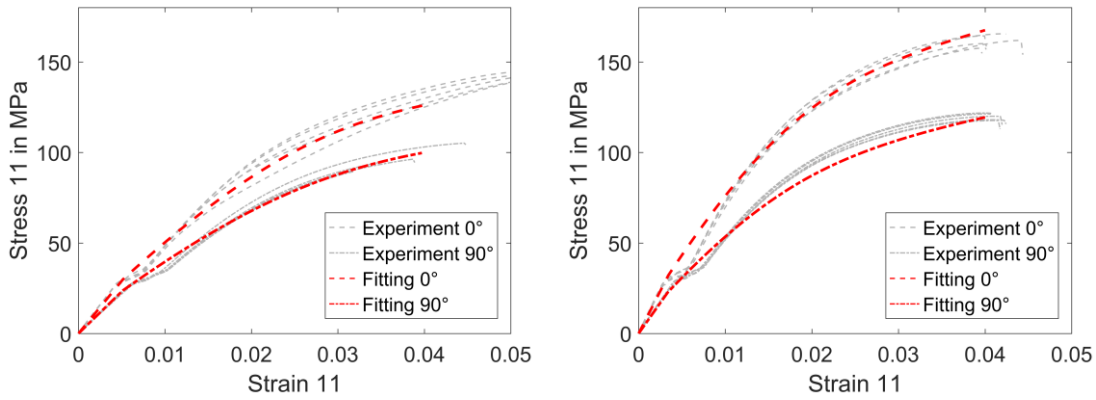


**Figure 2.** Comparison of experimental and fitted uniaxial stress strain curves for PA6GF30 (left) and PA6GF50 (right).

## 3. Numerical Multiscale Analysis and Validation

For the validation of the proposed multiscale approach, we perform a virtual three point bending test and compare it with experimental results. The test set-up and the corresponding virtual model are shown in Figure 3. The geometry of the structure and the injection mold have been developed in previous studies [6]. The geometry is manufactured by injection molding using PA6GF30 and PA6GF50, respectively with the process settings in Table 1.

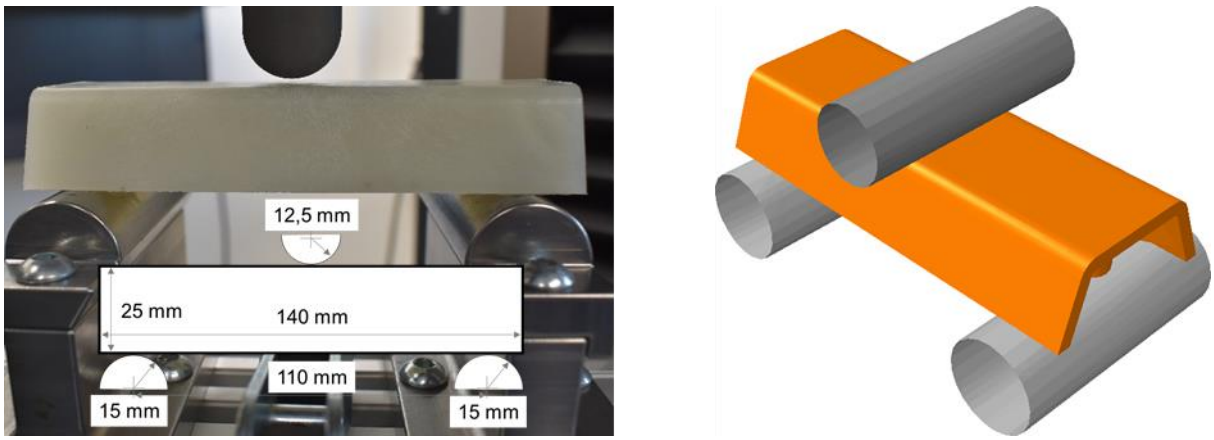


**Figure 3.** Three point bending test of a fiber reinforced 3D structure: experimental set-up (left) and virtual model (right).

The specimen has a total length of 140 mm. The radius of the supports is 15 mm and the span width is 110 mm. The impactor of radius 12.5 mm is placed in the center between the supports. During testing, it is moved downwards with a testing speed of 5 mm/min. In accordance with section 2, the experimental tests are carried out for both types of SFRP. For virtual testing, the fill analysis to determine the fiber orientation is combined with the structural finite element analysis.

### 3.1 Fill Analysis

In order to compute the fiber orientation, a computational analysis of the injection molding process using AUTODESK MOLDFLOW is carried out. The simulation is based on a rheological model for the flow properties of the melt. Due to the flow direction, the orientation of the glass fiber reinforcement can be determined. In this contribution, we use the Folgar-Tucker model [7,8] for the evaluation of the fiber orientation tensor. Accordingly, the time rate of change of fiber orientation is described by the fluid flow of the melt and the geometry of the inclusions. The fiber interaction is described phenomenologically by an additional scalar coefficient. For the fill analysis, the process parameters listed in Table 1 are applied as boundary conditions. The injection gate is located in the center of the component. The fill time and resulting fiber orientation are shown in Figure 4.

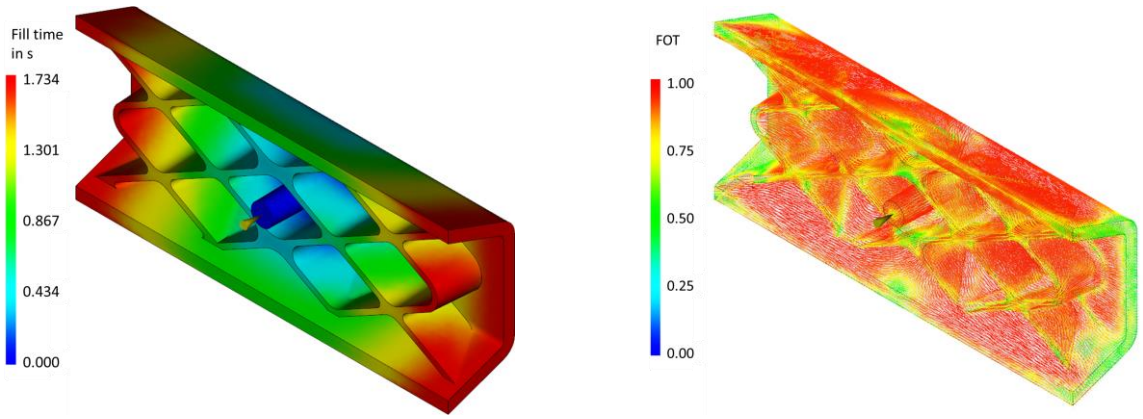


**Figure 4.** Results of the fill analysis of the 3D geometry:
fill time (left) and estimated fiber orientation (right).

### 3.2 Finite Element Analysis

For the structural analysis, the fiber orientation is mapped onto the finite element mesh using DIGIMAT. The supports and the impactor are modelled as analytical rigid surfaces according to the experimental set-up. The SFRP component is discretized by quadratic tetrahedral elements with an average element length of 2 mm. Due to the quasi-static loading, we use an implicit integration scheme for the elasto-plastic material formulation in ABAQUS/STANDARD. The material parameters from Table 2 obtained from the material characterization are used for the simulation.

In Figure 5, the resulting load deflection curve for the virtual three point bending test is compared with experimental results. In the diagram, the reaction force measured at the impactor is plotted over its displacement. The experimental results show a variation in the structural performance due to process induced voids, weld lines as well as defects on the surface. However, the computed load deflection curves for the presented geometry show good agreement with the experimental results for both materials. Comparing PA6GF30 and PA6GF50, an embrittlement due to higher fiber mass fraction is observable. The maximum load of the PA6GF50 specimen is about 30% larger than for PA6GF30.

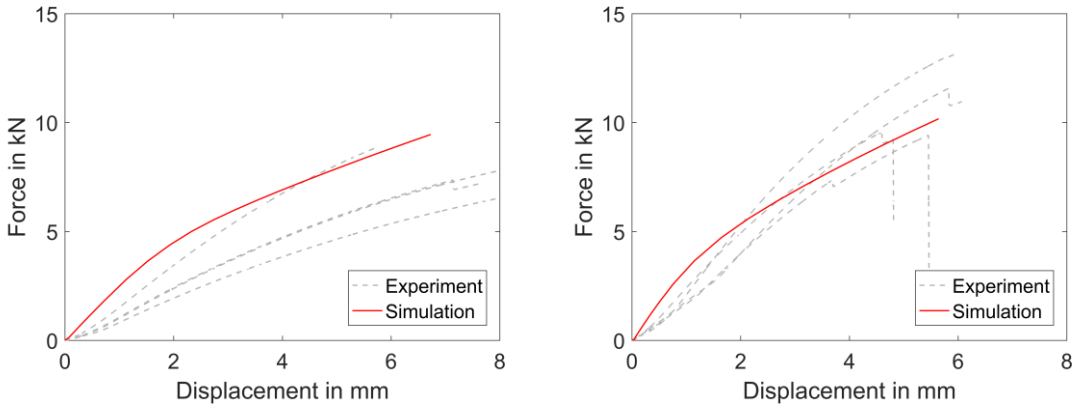


**Figure 5.** Comparison of experimental and computational load deflection curves for PA6GF30 (left) and PA6GF50 (right).

In Figure 6, the computational results of the virtual three point bending test are displayed for the PA6GF30 specimen. The accumulated plastic strain is plotted for an impactor displacement of 6 mm. The largest plastic strain occurs in the center line of the specimen according to the mechanical loading. Especially in the corner of the fins, plastic strain clusters are observable which corresponds to the failure pattern in the experimental tests. Furthermore, comparing the plastic strain distribution with the computed fiber orientation tensor in Figure 6 the plastic deformation correlates with the fiber orientation. The green elements indicate areas where no preferred fiber direction is present. Hence, the strength of the material is lower in those areas and consequently, the plastic deformations increase.

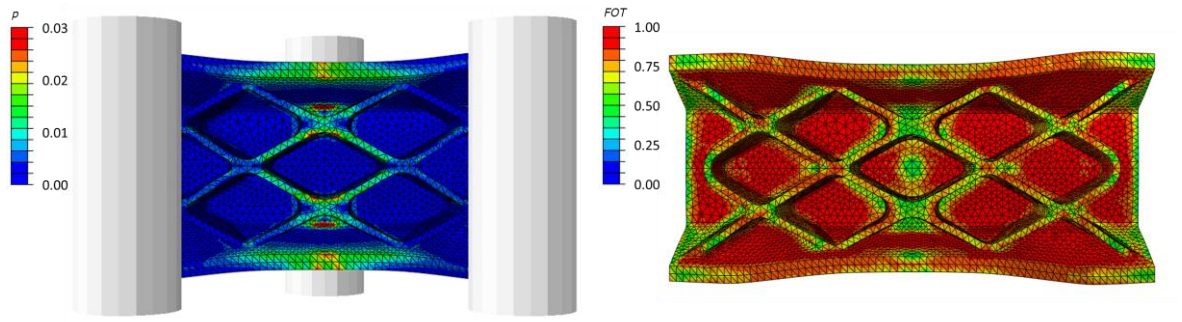


**Figure 6.** Accumulated plastic strain in the 3D geometry for PAGF30 at 6 mm displacement (left) and the corresponding fiber orientation in deformed the finite element mesh (right).

## 4. Hybridization with Surface Structured Metal Sheets

The presented geometry is extended by an in-mold connection with a structured sheet metal insert. In Figure 7, the hybrid component is depicted. It consists of the same injection mold as the specimen investigated in section 4. During the injection molding process, the metal sheet is formed by the injection and holding pressure from a plane geometry into the 3D geometry. Thus, the melt acts as action medium for the end-contour forming of the metal sheet. The resulting hybrid structure of the fiber reinforced plastic combined with a sheet metal insert is bonded by form closure effects as depicted in Figure 7. Previous studies have shown, that structured surfaces can increase the bond strength in comparison to conventional drilled holes to achieve form closure [9]. In addition, the

integration of surface structured metal sheets into the injection molding process provides and integrated process suitable for the line production of multimaterial lightweight components.

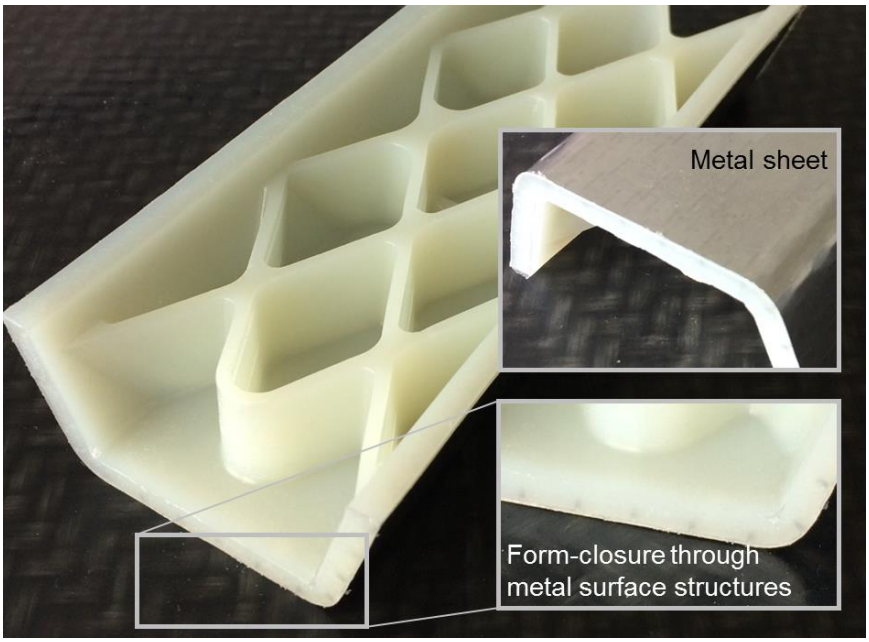


**Figure 7.** Hybrid structure of a mold integrated formed and bonded sheet metal and injection molded fiber reinforced plastic.

## 5. Conclusion

The presented multiscale approach is capable of representing the experimental characteristics of SFRP. Tensile specimen cut out of a plane geometry are used for material characterization. Based on the experimental data, an anisotropic elasto-plastic material model is parametrized and validated by a three point bending test of a lightweight demonstrator. The computational results show good agreement with experimental data. However, fracture criteria and the influence of welding lines have to be investigated and evaluated more deeply in further studies in order to improve the accuracy of virtual testing of composites. Furthermore, we are able to integrate an surface structured sheet metal into the injection molding process to obtain a hybrid composite. The resulting bond is given by form-closure effects between the two material classes.

## Acknowledgments

Funding of the research program “MOBILISE” by MWK Niedersachsen is gratefully acknowledged.

## References

[1] S. Nemat-Nasser and M. Hori. *Micromechanics. Overall properties of heterogeneous materials*. Elsevier, Amsterdam, 1999.

[2] J. D. Eshelby. The Determination of the Elastic Field of an Ellipsoidal Inclusion, and Related Problems. *Proceedings of the Royal Society A: Mathematical, Physical and Engineering Sciences*, 241:376–396, 1957.

[3] T. Mori and K. Tanaka. Average stress in matrix and average elastic energy of materials with misfitting inclusions. *Acta Metallurgica* 21(5):571–574, 1973.

[4] D. Gross and T. Seelig. *Fracture mechanics. With an introduction to micromechanics*. Springer, Berlin, 2011.

[5] G. Lielens. *Micro-macro modeling of structured materials*. PhD Thesis, 1999

[6] T. Gebken, M. Kühn, T. Seemann, R. van der Auwera, J. Steinberg. Prozessentwicklung für den hybriden Leichtbau am Beispiel einer endlosfaserverstärkten Aluminium-FVK-Struktur, *Symposium Hybrider Leichtbau, Wolfsburg*, 2016.

[7] F. Folgar and C.L. Tucker. Orientation Behavior of Fibers in Concentrated Suspensions. *Journal of Reinforced Plastics and Composites* 3(2):98–119, 1984.

[8] J. Wang, J.F. O'Gara and C.L. Tucker: An objective model for slow orientation kinetics in concentrated fiber suspensions: Theory and rheological evidence. *Journal of Rheology* 52(5): 1179–1200, 2008.

[9] K. Dröder, M. Brand, T. Gebken, M. Kühn and M. Böl. Increasing the interlocking effect between metal and FRP by mechanical undercuts. *International Journal of Automotive Composites* 2(3-4):316–329, 2016.